NUREG/CR-2023
PUR-101
R3

Modelling Hot-Pressing of UO_2

Manuscript Completed: August 1980
Date Published: March 1981

Prepared by
A. A. Solomon, K. M. Cuchran, J. A. Habermeyer

School of Nuclear Engineering
Purdue University
West Lafayette, IN 47907

Prepared for
Division of Reactor Safety Research
Office of Nuclear Regulatory Research
U.S. Nuclear Regulatory Commission
Washington, D.C. 20555
NRC FIN B6313

ABSTRACT

Final stage isostatic hot-pressing of nearly stoichimetric UO_2 was investigated. The rate of hot-pressing is linearly dependent on the pressure driving force $F = P + \frac{2\gamma}{r} - p$, where P and p are the external and internal pressures respectively, γ is the average surface energy and r is average pore radius. The apparent activation energy for hot-pressing agrees with that for U bulk diffusion. Grain growth during hot-pressing follows $d \propto t^n$, where d is the grain diameter, t is time and $n \simeq 0.2$. Grain size is also a function of temperature at constant density. The results indicate that Nabarro-Herring creep is the controlling mechanism of hot-pressing over the range of variables investigated, although the applicability of this model is questioned. The results also show that sintered UO_2 can entrap gas that can lead to swelling.

For modelling purposes, the isostatic hot-pressing of UO_2, under the conditions investigated, is best described by,

$$\frac{1}{V}\frac{dV}{dt} = \frac{A_2}{d^2}\left[\frac{1-\rho}{\rho}\right](\exp - Q/RT)\ F$$

where, $\frac{1}{V}\frac{dV}{dt}$ is the volumetric strain-rate in sec^{-1}, $A = 8 \times 10^3$, d is in μm, ρ is the relative density, Q = 480 kJ/g-mole, RT has its usual meaning, and F is in Pascals.

TABLE OF CONTENTS

List of Figures

MODELLING HOT-PRESSING OF UO_2

I. Introduction

The dimensional stability of ceramics under combined loads and high temperatures has assumed increasing importance as more ceramics are used as structural materials in energy-related technologies. Most engineering ceramics contain some residual porosity, so hot-pressing or densification under external pressure both during fabrication and in service is of considerable interest. Hot-pressing is especially important in oxide nuclear fuels because ∿5 to 10% porosity is intentionally incorporated in the fuel to accommodate fission products. Hot-pressing can occur by interaction with the fuel cladding or under the initial fuel pin pressure and released gas pressure.†

Surprisingly, there has been very little quantitative study of the hot-pressing behavior of high density UO_2 relevant to nuclear fuels. Kaufman[1] studied the hot-pressing of UO_2 of 82 to 86%TD at 1850°C and ∿39MPa using a vacuum hot-press and a single-action, graphite, punch and die (lined with tungsten to minimize contamination). In such an arrangement, die wall friction and specimen contamination are uncertain. Using only initial and final densities, he deduced that the linear strain-rate, $\dot{\varepsilon}$, is given by,

$$\dot{\varepsilon} = A\,\sigma^{n} \tag{1}$$

where A is a constant, σ is the applied stress, and n = 4.5. The constant A is usually assumed to contain temperature and structural parameters (porosity, grain size, point defect concentrations). However, the total driving force, F, for volume change is a function of the external pressure, P, the internal pore pressure, p, and the surface tension term $2\gamma/r$, viz.,

$$F = P - p + 2\gamma/r \tag{2}$$

---

†During fissioning, fuels may undergo hot-pressing at very low temperature under the same driving forces as discussed here (to be published by A.A.S.)

where γ is an average surface energy and r is the radius of an assumed spherical pore.[2] In Kaufman's experiments, p was presumably neglible in the vacuum hot-press, but the sintering term, $2\gamma/r$, was neglected.

A number of workers[3,4,5] have been primarily interested in fabricating high density UO_2 and $(U, Pu)O_2$ by hot-pressing in punch-and-dies, by hot isostatic pressing or by hot-pressing during a phase change.[6] Generally, these data do not permit accurate analysis of the stress or temperature dependencies, but Hart[3] found for his experiments on UO_2 at 900^oC, that n varies from 1.5 to 4 for $13.8 < \sigma < 41.4$ MPa. Similarly, he found n = 2 to 3 for the data of Warren and Chaklader.[6] Hart[3] and Routbort, et al.[7] have also found that $n > 1$ for $(U, Pu)O_2$. Such results are difficult to rationalize with simple theory[2]. Contamination from die materials, stoichiometry control, and lack of grain growth measurements during testing have been additional complications.

The porosity dependence of hot-pressing has received considerable attention, and numerous empirical and analytical forms have been proposed. Although these functions tend to merge at high density, they become very important as theoretical density is approached.

The temperature dependence of hot-pressing is usually given by an Arhennius factor, $e^{-Q/RT}$, where Q is the apparent activation energy for bulk or grain-boundary diffusion and RT has its usual meaning. Unfortunately, there are essentially no well-controlled measurements of specimen stoichiometry and Q for UO_2 hot-pressing.

The purpose of the present investigation, therefore, was to measure isostatic hot-pressing rates in well-controlled experiments on well-characterized high density UO_2, and to identify the rate-controlling mechanisms in terms of known pressure driving forces that are relevant to nuclear reactor fuels.

II. Experimental

A. Materials and Preparation.

The starting ADU-UO_2 powder* had a reported+ Fisher sub-sieve size of 3.16 μm, a bulk density of 2.17 g/cc, a surface area of 6.73 m^2/gm and a density of 99.3%. Examination under scanning electron microscopy, SEM, revealed that the powder was highly agglomerated and apparently much finer (∿0.12μ). An analysis of major impurities is given in Table 1.

Pellets were first formed at 0.7 MPa in a double-action punch and die which provided equal displacement of each punch so that a uniform initial geometry was obtained. No binders, lubricants or pore formers were used. The pellets were then isostatically compressed at 345 MPa to a density of ∿50%TD to obtain the most uniform green density possible. A small amount of hourglassing was found after isostatic pressing.

Batches of specimens were then pre-sintered in flowing Ar-5%H_2 in a 99.8% pure alumina tube at temperatures from 1100°C to 1510°C for 0.5 to 67 hours. After sintering, immersion density measurements were performed in ethyl alcohol‡ to determine pore closure behavior for the subsequent hot-pressing experiments. Two or more density measurements were made on each specimen, and the results were averaged. The immersion densities were reproducible within ± ½%. For the hot-pressing experiments, all of the specimens were pre-sintered at 1510°C for 3 hours in flowing Ar-5%H_2.

Ceramography and SEM examination were performed on pre-sintered specimens and hot-pressed specimens. Specimens were mounted in epoxy and polished to 1 μm diamond. Interference microscopy revealed minimum edge rounding after final polishing. Specimens were cooled under pressure after a hot-pressing experiment to maintain the pore morphology.

Pellet stoichiometry was measured by reduction in 38% CO/62%CO_2 and by ignition to U_3O_8 in air, both at 800°C for 12 hours.

B. Hot-Pressing Experiments

The hot-pressing experiments were carried out in a special hot isostatic pressurization system, Fig. 1, described elsewhere.[8] A thoria-dispersed tungsten pressure vessel was used, which yielded < 1°C temperature variation in the specimen at 0.1 MPa pressure. This was measured by moving a W/5%Re vs. W/26%Re thermocouple through a hollow dummy specimen. The tungsten pressure vessel served to establish the oxygen potential since traces of condensed blue tungsten oxide were seen at the cooler regions of the pressure vessel after testing.

In a typical experiment, the initial atmosphere was set by first evacuating and back-filling the pressure vessel three times at room temperature to 0.14 MPa with dry Ar-5%H_2; then increasing temperature linearly in 1 hour to 800°C; holding at 800°C for 1 hour during which a second evacuation and back-filling was performed with Ar-5%H_2; and finally increasing temperature linearly to the test temperature in 10 minutes and evacuating and back-filling a third time with Ar-5%H_2, at the test temperature. The evacuation and back-filling was performed to eliminate water and other adsorbates from the static pressure vessel atmosphere. The specimen was pressurized with ultra-high-purity argon 30 min. after reaching Set Point on the programmer. The argon was passed through a drier and Zr chip getter-furnace at 800°C before being compressed by the diaphragm pump and fed to the pressure vessel.

An automatic microprocessor furnace programmer*** was used with an SCR power supply and a $MoSi_2$ element furnace to accurately program and control the specimen temperature to within $\pm$ 1°C in 24 hours. Since UO_2 equilibrates chemically in ~ 1 hour at 800°C[9], equilibration should have been very rapid at the test temperature of 1410°C.

Calibration experiments on the TD tungsten vessel were used to correlate the temperatures in a hollow dummy specimen within the vessel, with the control thermocouple outside the vessel, Fig. 1. For temperature cycling experiments, the specimen temperature was found to change in <2 minutes following an abrupt change in the control temperature. The

specimen also reached the test temperature in <15 min. after the programmer reached the Set Point when heating from 800°C to 1410°C in 10 minutes.

Pressure changes were made in 5 to 10 seconds either by filling from a high pressure accumulator or by releasing gas to the outside. The pressure was measured by a Heise Guage and a strain-guage pressure transducer[++], both within 0.1% accuracy. Pressure was controlled within ± .7MPa during an experiment by bleeding gas from the accumulator as needed.

III. Results

A. Porosity Evolution and Sintering Behavior

Sintering experiments were carried-out in order to examine the evolution of the microstructure and determine the point of pore closure during sintering prior to hot-pressing. Specimens were sintered in flowing dry Ar-5%H_2 in a high purity alumina tube at 1100°C to 1510°C for 0.5 to 67 hours. Individual specimens in a batch were suspended in Al_2O_3 baskets that could be withdrawn from the hot-zone at various times. The O/M ration after sintering was measured to be 2.004.

Immersion density measurements after sintering revealed typical porosity evolution with pore closure at ∿ 91%TD, Fig. 2. The hot-pressing experiments were carried out at >94%TD, at which essentially all the pores were closed.

Microstructural examination of the porosity indicated that the agglomerates present in the starting powder were not broken up by the 345 MPa isostatic compaction. Fig. 3 shows that the agglomerate porosity coarsens significantly from ∿90 to 95%TD, leaving pockets of large pores as well as very fine pores seen by SEM, Fig. 4.

B. Hot-pressing Experiments and Results

The hot-pressing experiments are listed in Table 2. Most of the

specimens were pre-sintered in flowing Ar-5%H_2 at 1511^{o}C for 3 hrs to ∿ 94%TD. Specimen #5-6 was sintered rapidly at high temperature within the pressure vessel as part of a compatibility experiment between magnesium zirconate, platinum, and tungsten and exhibited unusual behavior.

(1) Pressure Dependence

The pressure dependence of hot-pressing in UO_2 was determined both by pressure cycling a single specimen at constant temperature and by hot-pressing a series of specimens, all pre-sintered identically, at various pressures. The former method has the advantage of eliminating specimen-to-specimen variations, but requires extrapolation to obtain the difference in strain-rate at a constant structure.

The density during an experiment, ρ, was calculated from the measured specimen length, ℓ, and the measured final immersion density using $\frac{\rho}{\rho_f} = (\frac{\ell_f}{\ell_f+\Delta\ell})^3$ where ℓ_f and ρ_f are the final length and density, respectively, and $\Delta\ell = \ell-\ell_f$. The final immersion density was averaged over two or more independent measurements. All of the constant pressure experiments conducted at 1410^{o}C are shown in Fig. 5, where least squares fits are indicated for all pressures except 13.79 MPa to avoid confusion. The test at the highest pressure exhibited leakage so the average pressure is indicated. The average initial sintering rate obtained during a half hour equilibration period prior to pressurizing the specimens is seen to be non-negligible.

When the strain-rates are plotted at constant density, Fig. 6, it is found that the strain-rate extrapolates to zero at a negative pressure, indicating that surface tension and perhaps internal pressure are contributing to the driving force.

Following Eq. 2, the intercept values represent the terms $\frac{2\gamma}{r}$ - p, both of which are functions of pore radius or specimen density as shown in

Fig. 7. Since, for ideal gas within the pores, $p \propto 1/r^3$, the increasing intercept is consistent with increasing values of p and density. If the values of the intercepts for each density are added to the external pressure, the resultant strain rate vs. pressure driving force, F, is essentially linear, Fig. 8.

The result of a typical pressure cycling experiment is shown in Fig. 9. Again, the sintering rate is seen to be non-negligible. The pressure dependence for these experiments was determined using $n = d\ln\dot{\varepsilon}/d\ln F$ for each of the pressure changes. To evaluate F, the $2\gamma/r-p$ term must again be estimated. This was done by assuming a linear $\dot{\varepsilon}$ vs. F relation and comparing the extrapolated sintering and hot pressing strain-rates at 10.35 MPa, and 93.3%TD, i.e., $\dot{\varepsilon}_1/\dot{\varepsilon}_2 = [P + (2\gamma/r-p)]/(2\gamma/r-p)$. This yielded a value of $2\gamma/r-p$ of 4.8 MPa at 93.3%TD which is consistent with the values determined by extrapolation, Fig. 7. Therefore, values of $2\gamma/r-p$ at other densities were taken from Fig. 7 to calculate F and n. The resultant n values indicated in Fig. 9 for each pressure change are consistent both with the value previously obtained of n=1 and with the assumed linear stress dependence.

(2) Temperature Dependence

To determine the temperature dependence of hot-pressing, temperature cycling was performed on individual specimens during hot-pressing, and a series of specimens were run at different temperatures. The temperature cycling experiment has the advantage that data is obtained on a single specimen and the uncertainty of possible variations in the grain size and the $(\frac{2\gamma}{r} - p)$ terms at different temperatures are avoided.

A typical temperature cycling experiment is shown in Fig. 10. The apparent activation energy, $Q = -Rd\ln\dot{\varepsilon}/d(1/T)$, was 480 kJ/g-mole from two series of cycling experiments.†

Comparing strain-rates for specimens at different temperatures and constant density yielded lower activation energies, ($\sim 290 \frac{kJ}{g\text{-mole}}$). However, at constant density the grain size varies with temperature, Fig. 11, so

†The small change in internal pressure with temperature has been neglected.

this activation energy is inaccurate. To normalize for the grain size would require knowledge of the strain-rate dependence on grain size which was not obtained. The grain size variation with temperature trend is such as to make the activation energy larger and in closer agreement with the temperature cycling experiments.

(3) Stoichiometry

Because of the very small weight changes involved in reducing the specimens in CO/CO_2 mixtures ($\sim$0.1 mg), it was decided that ignition to U_3O_8 was a more reliable method of measuring specimen stoichiometry. The measured O/M value after hot-pressing was 2.004 $\pm$ .001. This value agrees well with equilibrium of tungsten and WO_2 and WO_3 at 1410°C.[10]

(4) Grain Growth

Grain growth during hot-pressing was important only for those experiments which follow the strain-rate change with time or density. The results of the pressure or temperature cycling experiments are thus not affected. In the tests conducted at various pressures but constant temperature, it is tacitly assumed that grain growth is not a function of pressure. However, as pointed out above, for the tests at constant pressure but variable temperature, one must investigate possible grain size variations at constant density.

Grain sizes were averaged over 10 random measurements of linear intercepts. Quoted values are the mean linear intercepts x 1.56[11]. The grain size, d, at 1410°C (including the 30 min preconditioning), increases with time, t, at 1410°C as $d \propto t^n$, where $n \cong 0.2$, Fig. 12.

(5) Entrapped Gas and Grain Size Effects

As mentioned earlier, specimen #5-6, exhibited intriguing results from two points of view. First, it was found that after hot-pressing some amount, when the specimen was unpressurized, it swelled under an apparent

internal pressure, Fig. 13.† Hot-pressing and swelling could then be performed alternately in an almost reversible manner (there was some reduction in rates with time). This behavior was in marked contrast to all other experiments in which hot-pressing, even to very high density >99%TD, did not lead to swelling when the specimen was unloaded.

The second effect of interest was that #5-6 exhibited higher strain-rate than the other specimens at the same density. Its grain size, Fig. 12, was also smaller, perhaps due to contamination. This would suggest that the hot-pressing strain-rate may be grain-size dependent, although other effects of impurities may also be possible.

(6) Microstructural Evolution During Hot-Pressing

The evolution of the microstructure during hot-pressing is shown in Fig. 14. The remnants of agglomerates present after sintering are seen to break up and disappear during hot-pressing. Examination of the open porosity before and after hot-pressing, Table 2, shows that the pores do not tend to open while under external pressure. Another point of interest is that most of the pores appear to be located within the grains, and the grains appear equiaxed.

IV. Discussion

The observed linear dependence of the strain-rate on driving force strongly suggests a mass transport process controlled by diffusion in UO_2 under the conditions investigated. The apparent activation energy for the creep of UO_2 is very sensitive to stoichiometry, but has been measured to be ∿313 kJ/g-mole for single crystals[12] and ∿250 kJ/g-mole for polycrystalline material[13], both of which are lower than the measured 480 kJ/g-mole. On the other hand, the activation energy for uranium self-diffusion in UO_2 single crystals is ∿460 kJ/g-mole.[14] Since, in the

†Recent sintering experiments under pressure have shown that UO_2 can entrap gas during heating which later causes swelling at temperature.

present work, the pores are largely intragranular, diffusion through the bulk would appear appropriate, and the activation energy for U diffusion agrees reasonably well with the measured value for hot-pressing.

The decrease in the values of $2\gamma/r-p$ during densification, Fig. 7, would suggest that an internal pore pressure does exist and increases as $1/r^3$ and offsets the increase in surface tension with density. From the results on Spec. #5-6, it is clear that gases can be entrapped during sintering. An attempt was therefore made to verify this by unloading a typical specimen hot-pressed to 99.6%TD, but no swelling was detected, perhaps because the rate was too low.

The good agreement between the pressure cycling and the constant pressure experiments would suggest that the deformation process is not history dependent, and therefore is not controlled by dislocation plasticity between the pores as suggested by Ashby[15].

A number of detailed models have been proposed to describe diffusion-controlled hot-pressing. When pores reside on grain boundaries, and mass transport occurs along the boundaries, Wilkinson[16] obtains

$$\left(\frac{1}{\rho}\frac{d\rho}{dt}\right)_b = \frac{9}{2}\frac{\delta D_B \Omega}{kTd^3}\left\{\frac{1}{[1-(1-\rho)^{1/3}]\rho}\right\} F \qquad (2)$$

where δ and D_B are the effective grain boundary "width" and diffusivity, respectively, d is the grain size, Ω is the atomic voluem and kT has its usual meaning. Note that $\dot{\rho} \neq 0$ at $\rho = 1$.

A similar result is obtained for bulk diffusion between pores located on boundaries and the grain boundaries,[16]

$$\left(\frac{1}{\rho}\frac{d\rho}{dt}\right)_v = 3\frac{D_v \Omega}{kTd^2}\left\{\frac{(1-\rho)^{1/3}}{\rho[1-(1-\rho)^{1/3}]}\right\} F \qquad (3)$$

where D_v is the bulk diffusion coefficient. Coble[17] assumed a more

relevant geometry in which pores were located within the grains and obtained an identical result, if it is assumed that $\rho = 1 - \frac{r}{d}^3$ and his correction of P to produce an "effective" P is omitted.

If power-law creep of the matrix is controlling and the uniaxial tensile creep rate of a fully dense specimen is given by $\dot{\varepsilon} = A\sigma^n$, then from Wilkinson and Ashby,[18]

$$\left(\frac{1}{\rho}\frac{d\rho}{dt}\right)_c = \frac{3}{2} A \frac{(1-\rho)}{[1-(1-\rho)^{1/n}]^n} \left(\frac{3F}{2n}\right)^n \qquad (4)$$

For n = 1, this reduces essentially to the result given by Murray et al.,[19]

$$\left(\frac{1}{\rho}\frac{d\rho}{dt}\right)_c = \frac{9}{4} A \left(\frac{1-\rho}{\rho}\right) F \qquad (5)$$

In order to test the validity of these models, the value of n = 1 was used from the present investigation, and the other parameters for UO_2, Table 3, were taken from Wilkinson.[16] The value of A for fully dense $UO_{2.004}$ was obtained from the results on polycrystalline UO_{2+x} at low stress by Seltzer et al.[13] Normalizations were made for density (95% to 100%TD) using their measured density dependence; for temperature, using their measured activation energy of 251 kJ/g-mole for $UO_{2.004}$; and for grain size using their measured d^{-2} dependence for low stress.

The results using Eqns. 2, 3, & 5 are shown in Fig. 15, where a hot-pressing experiment at 13.8MPa is examined. The models for grain boundary and bulk diffusion are seen to be 2 to 3 orders of magnitude lower than the measured hot-pressing rates. If the fraction of the pores lying on the grain boundaries is considered, the discrepancy would be even larger. The power-law creep model for n = 1 appears to fit the data better, perhaps because it is based on measured creep rates and

also because it fits the situation of isolated pores far from grain boundary sinks. Over the range of densities and grain sizes investigated, all functions describe the decrease in the strain rate during hot-pressing reasonably well, but the boundary diffusion model shows somewhat more variation than measured.

This result is especially interesting in view of the conclusion by Routbort, et al.[7] that bulk diffusion controls hot-pressing in $(U,Pu)O_2$, although they find a factor of 30 deviation in some cases. It may be that the diffusional creep data for $(U,Pu)O_2$ do not permit an accurate value of A to be determined, or that die wall friction or contamination may have been important.

On the basis of Fig. 15, it would appear that Nabarro-Herring viscous creep controls final stage hot-pressing in UO_2 over the range of variables investigated. The model fits the observed microstructures, gives the measured pressure and temperature dependencies, describes the decrease in strain-rate with density and, moreover, gives the proper magnitude. This model, however, is most appropriate for fine-grained material surrounding relatively large pores. When the reverse is true, as in the present use, it is difficult to see why vacancy fluxes between more distant grain boundaries should be rate-controlling rather than fluxes between pores and boundaries. Even if fluxes between boundaries control, the presence of the pores should affect the stress state and boundary tractions in the Nabarro-Herring creep model in order to close the pores. An additional test would be to further verify the $1/d^2$ grain size dependence and porosity dependence over larger density ranges during hot-pressing, and to investigate variations in stoichiometery, since the creep rate is so sensitive to stoichiometry variations.

Another extension of this study would be to evaluate the surface tension and internal pressure terms. The former could best be determined by measuring the average pore size in a material that exhibits uniform pore size. Internal pressures could be evaluated by swelling experiments, as has been done in ZnO.[20]

UO_2 hot-pressing has been modelled by the MATPRO - Version 11 (Rev. 1)[21]

fuel modelling code under the subroutine FHOTPS. Use of the hot-pressing relation at low stress,

$$\dot{\varepsilon} = \frac{A_1 \sigma \exp(-Q_1/RT)}{(-0.877 + \rho)d^2}$$

and,

$$Q_1 = 17.88 \left\{ \exp\left[\frac{-20}{\ln(x-2)} - 8\right] + 1 \right\}^{-1} + 72.12 \qquad (6)$$

yields a strain-rate ~ 7.5 orders of magnitude too high. This discrepancy appears to arise from an error in the units of Q which are stated in kJ/g-mole, but appear to be in kcal/g-mole. When units of kcal/g-mole are used, the predicted strain-rates are 1.2 orders of magnitude lower than the measured values. The low stress expression was used because the applied stress was less than the transition stress for dislocation creep,[13] and because of the measured linear dependence of $\dot{\varepsilon}$ on F.

From our results the best empirical relationship for hot-pressing is,

$$\frac{1}{V}\frac{dV}{dt} = \frac{A}{d^2}\left[\frac{1-\rho}{\rho}\right] (\exp - Q/RT)\, F$$

where, $\frac{1}{V}\frac{dV}{dt}$ is the volumetric strain-rate in sec^{-1}, $A = 8 \times 10^3$, d is in μm, ρ is the relative density, Q = 480 kJ/g-mole, RT has its usual meaning, and F is in Pascals.

V. Summary and Conclusions

(1) The isostatic hot-pressing rate in UO_2 is linearly proportional to the pressure driving force $P + \frac{2\gamma}{r} - p$.

(2) Both pressure cycling and tests at different pressures yield the same pressure dependence indicating no history dependence in the flow

process as might be present for dislocation controlled flow.

(3) The apparent activation energy for hot-pressing is 480 kJ/g-mole which agrees best with the volume diffusion of uranium in UO_2.

(4) Grain growth during hot-pressing follows a relation $d \propto t^n$ where $n \simeq 0.2$.

(5) The grain size at constant density is temperature dependent.

(6) Under conditions of rapid sintering and impurity contamination, UO_2 can entrap significant gas pressures which subsequently can cause swelling.

(7) Models for hot-pressing by vacancy fluxes between pores and grain boundaries underestimate the hot-pressing rates by 2 to 3 orders of magnitude.

(8) The hot-pressing of $UO_{2.004}$ at pressures from 0.14 to 27.6MPa and temperatures from 1360 to 1460°C was quantitatively best described by Nabarro-Herring creep of the matrix material surrounding the pores. However, this model is questioned on theoretical grounds. Also, the agreement may be fortuitous because actual creep data are used rather than highly uncertain activation parameters.

Table 1

CHEMICAL AND PHYSICAL DATA

ADU - UO_2 (depleted)

P. O. No. Q04091
Lot No. 450728

	Specification	Y-12 Analysis
Uranium Content (wt%)	86.0 min.	86.6826
Isotopic Analysis (wt%)		
U-234	-	< 0.010
U-235	Depleted	0.195
U-236	-	< 0.010
U-238	-	99.884

Impurities (ppm U basis)

Element	Max.	ppm
Aluminum	100	15.0
Boron	---	0.2
Carbon	150	65.0
Calcium + Magnesium	125	< 12.0
Cadmium	---	< 0.1
Chlorine + Fluorine	125	3.0
Chromium	200	< 2.0
Cobalt	100	< 1.0
Copper	---	10.0
Hafnium	---	< 0.1
Iron	400	200.0
Lithium	---	< 0.2
Manganese	---	10.2
Nickel	200	2.0
Nitrogren	200	18.0
Silicon	200	40.0
Silver	---	< 1.0
Tantalum	---	1.0
Titanium	---	1.0
Tungsten	---	7.0
Vanadium	---	0.6
Zinc	---	3.0
Rare Earth		
Dysprosium	---	< 0.10
Europium	---	< 0.06
Gadolinium	---	< 0.08
Samarium	---	< 0.10
TOTALS	1500 max.	< 393.0

Table 1 (cont.)

CHEMICAL AND PHYSICAL DATA

P. O. No. Q04091

Lot No. 450728

ADU-UO_2 (Depleted)

	Specification	Y-12 Analysis
Moisture Content (wt%)	0.80 max.	0.80
O/U Ratio (calculated %)	---	2.11
Particle Size	Pass through 20 Mesh Screen	Pass through 50 Mesh Screen
Avg. Particle Size (by Fisher sub-sleve-sizer)	---	3.16μ
Density (Toluene)(gm/cc)	---	10.617
Density (Bulk)(gm/cc)	---	2.11
Surface Area (M^2/gm)	---	6.73
Porosity (%)	---	0.725

Table 2. Hot-Pressing Experiments

	Pre-sinter Conditions			Hot-Press. Conditions				
Spec.	$^{o}T_{C}$	t min	%TD	% Open Por.	$^{o}T^{+}_{C}$	P^{*} MPa	%TD	% Open Por.
5-6	1600	420	94.9	0.1	1410	6.90	91.1	1.1
5-3	1300	4000	93.6	1.5	1410	6.90	90.8	2.6
3-6	1511	182	95.0	1.0	ΔT	ΔP	94.9	3.1
3-5	1511	30	91.5	4.7	ΔT	20.69	98.1	0.7
7-10	1511	172	94.3	1.6	1410	ΔP	96.9	2.0
7-12	1511	172	94.2	1.2	1410	ΔP	98.3	.7
7-14	1511	172	95.0	0.7	1410	20.69	98.7	0.3
7-9	1511	172	93.2	1.5	1410	6.90	97.4	0.6
7-2	1511	172	93.8	2.3	1410	13.79	98.2	0.3
7-5	1511	190	93.7	1.1	1410	27.59	98.4	0.6
10-6	1511	190	94.9	1.1	1410	3.45	97.4	0.8
10-1	1511	190	95.1	0.9	1410	27.59	98.3	0.5
10-4	1511	190	95.2	0.9	1410	.14	96.5	0.7
10-5	1511	190	95.2	0.7	1353	20.69	98.4	0.3
10-2	1511	190	94.9	1.0	1460	20.69	95.9	0.4
10-7	1511	190	94.6	1.4	1460	20.69	99.6	0.3
7-1	1511	190	95.0	1.0	1410	3.45	96.5	0.3

$^{+}$ΔT is a variable temperature test.

*ΔP is a variable pressure test.

Table 3. UO_2 Parameters from Ref. 16

Atomic Vol.	≡	Ω	$= 4.09 \times 10^{-29} m^3$
D_o for volume diffusion	≡	D_{ov}	$= 1.2 \times 10^{-5} m^2/sec$
δD_o for boundary Diffusion	≡	δD_{ob}	$= 2.0 \times 10^{-15} m^3/sec$
Activation Energy, boundry diffusion	≡	Q_b	= 293 kJ/mole
Activation Energy bulk diffusion	≡	Q_v	= 452 kJ/mole

Footnotes

*Furnished through the courtesy of Exxon Nuclear Corporation

+Oak Ridge National Laboratory

‡Usi ⌟ ASTM #132

**Plastimet, Buehler Corp., 2120 Greenwood St., Evanston, IL 60204

***Iveron Pacific Corporation, Model 2100A, 1152 Morena Blvd., San Diego, CA 92110

++Sensotec Corporation, Model TJE, 1200 Chesapeake Avenue, Columbus, OH 43212

Acknowledgement

The authors would like to express their appreciation to the Nuclear Regulatory Commission for support under Contract #478231.

References

(1) S. F. Kaufman, "The Hot-Pressing Behavior of Sintered Low-Density Pellets of UO_2, ZrO_2-UO_2, ThO_2 and ThO_2-UO_2" WAPD-Tm 751, (May 1969).

(2) A. A. Solomon and F. Hsu, pp 485-502 in Sintering Processes, Ed. by G. C. Kuczynski, Plenum, New York, (1980).

(3) P. E. Hart, "Fabrication of High-Density UO_2 and $(U_{0.75}\ Pu_{0.25})\ O_2$ by Hot Pressing," J. Nucl. Mater., 51 (1974) 199-202.

(4) B. Schaner, in: Uranuim Oxide: Properties and Nuclear Applications, ed. J. Belle (USAEC, 1961) p. 30.

(5) I. Amato, R. Colombo and A. Balzari, J. Nucl. Mater., 20 (1966) 210.

(6) I. H. Warren and A. C. D. Chaklader, "Reactive Hot Pressing of Non-stoichiometric Uranium Dioxide," Met Trans., 1 (1970) 199-205.

(7) J. L. Routbort, J. C. Voglewede and D. S. Wilkinson, "Final Stage Densification of Mixed Oxide Fuels " J. Nucl. Mater., 80 (1979) 348-355.

(8) R. C. Abbott and A. A. Solomon, "A New Technique to Study Effects of Internal and External Pressure in Ceramics", Am. Ceram. Soc. Bull., 58 (4) 470-72 (1979).

(9) C. E. McNeilly and T. D. Chikalla, "Determination of Oxygen/Metal Ratios for Uranium, Plutonium, and (U, Pu) Mixed Oxides," J. Nucl. Mater., 39 (1971) 77-83.

(10) Contributions to the Data on Theoretical Metallurgy, XIV Entropies of the Elements and Inorganic Compounds, by K. K. Kelley and E. G. King, Bureau of Mines, Bull. 592, (1961).

(11) M. I. Mendelson, "Average Grain Size in Polycrystalline Ceramics," J. Amer. Ceram. Soc., 52 (8) 443-46 (1969).

(12) M. S. Seltzer, A. H. Clauer and B. A. Wilcox, "The Influence of Stoichiometry on Compression Creep of Uranium Dioxide Single Crystals," J. Nucl. Mater., 44 (1972) 43-56.

(13) M. S. Seltzer, A. H. Clauer and B. A. Wilcox, "The Influence of Stoichiometry on Compression Creep of Polycrystalline UO_{2+x}," J. Nucl. Mater., 44 (1972) 331-336.

(14) M. S. Seltzer, J. S. Perrin, A. H. Clauer, and B. A. Wilcox, "Review of Out-of-Pile and In-pile Creep of Ceramic Nuclear Fuels," Battelle Memorial Institute Report #BMI-1906, (July 1971).

(15) M. F. Ashby, C. Gandhi and D. M. R. Taplin, Acta Met, 27, (1979) 699.

(16) D. S. Wilkinson, Ph.D. Thesis, University of Cambridge (1978).

(17) R. L. Coble, "Diffusion Models for Hot Pressing with Surface Energy and Pressure Effects as Driving Forces," J. Appl. Phys., 41 (12) (1970) 4798-4807.

(18) D. S. Wilkinson and M. F. Ashby, "Pressure Sintering by Power Law Creep," Acta Met, 23 (1975) 1277-1285.

(19) P. Murray, D. T. Livey, and J. Williams, "The Hot Pressing of Ceramics," in Ceramic Fabrication Processes, W. D. Kingery, Ed., pp. 147-171, The M. I. T. Press, Cambridge Mass. (1958).

(20) A. A. Solomon and F. Hsu, "Swelling and Gas Release in ZnO," J. Amer. Ceram. Soc., 63 (7-8) (1980) 467-474.

(21) MATPRO - Version 11 (Revision 1). A Handbook of Materials Properties for Use in the Analysis of Light Water Reactor Fuel Rod Behavior, NUREG/CR-0497 TREE-1280, Rev. 1 (Feb. 1980).*

*Available for purchase from the NRC/GPO Sales Program, U.S. Nuclear Regulatory Commission, Washington, DC 20555, and the National Technical Information Service, Springfield, VA 22161.

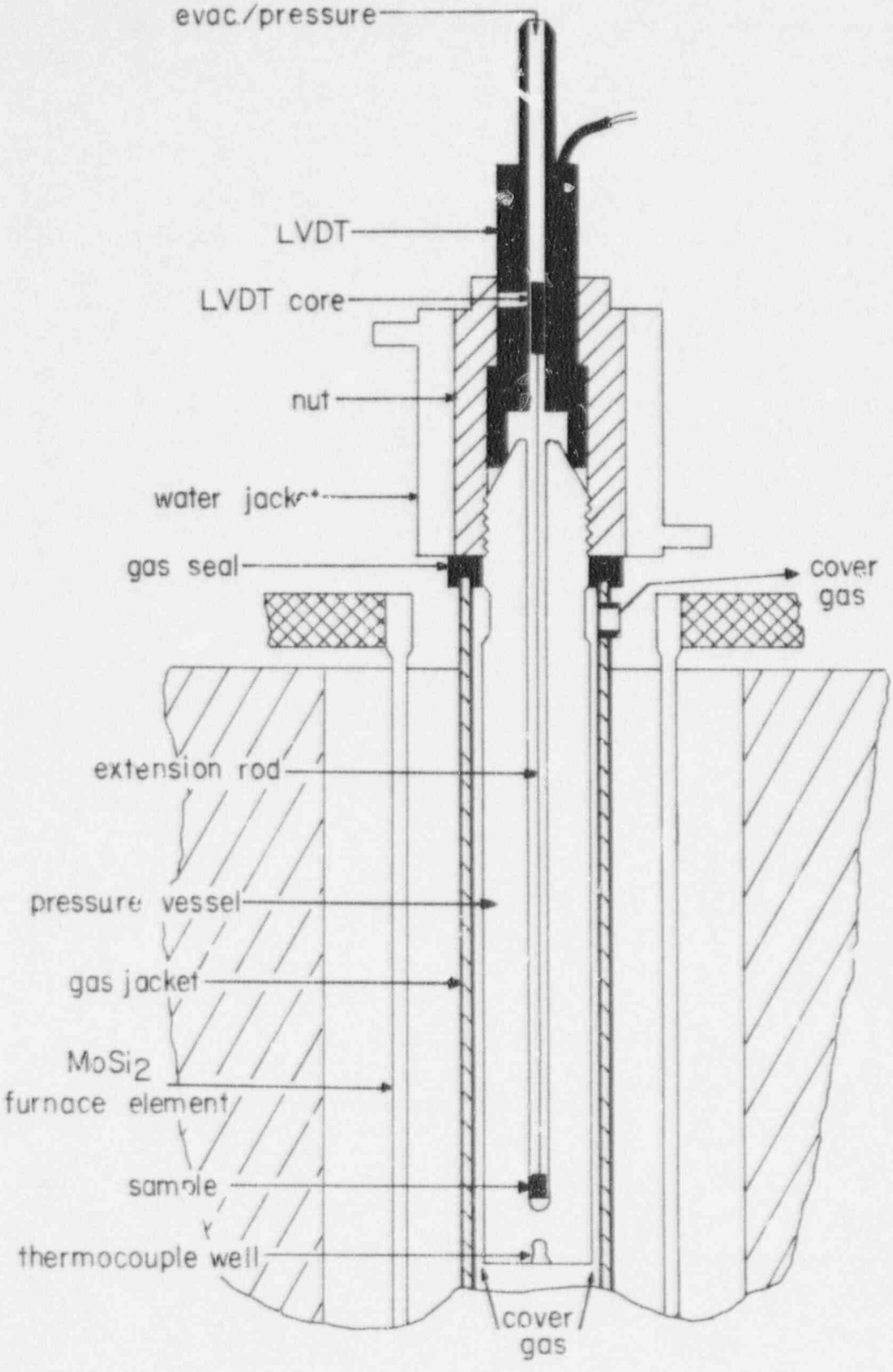

Fig. 1. Isostatic pressurization system

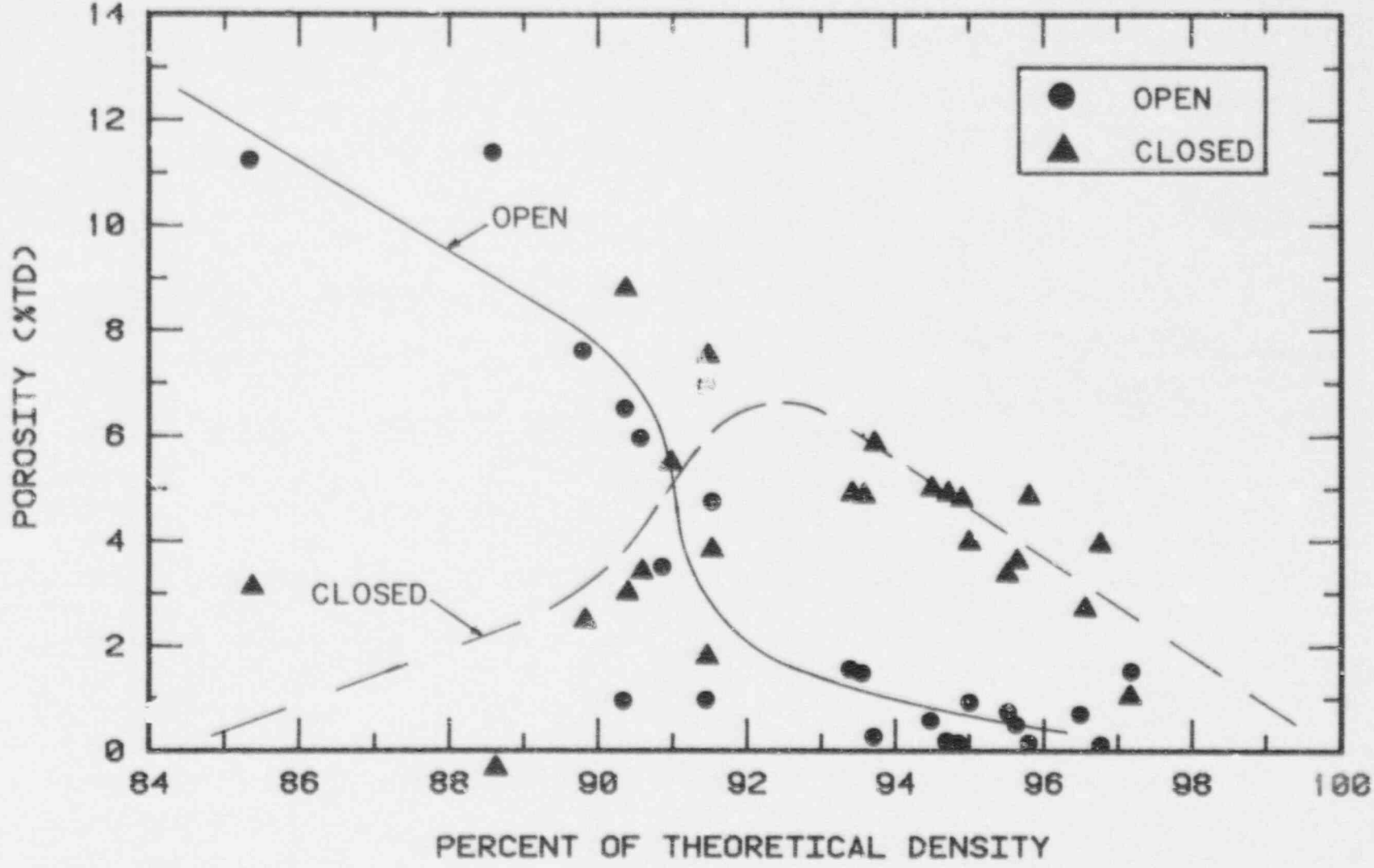

Fig. 2. Pore closure in UO_2 from immersion density

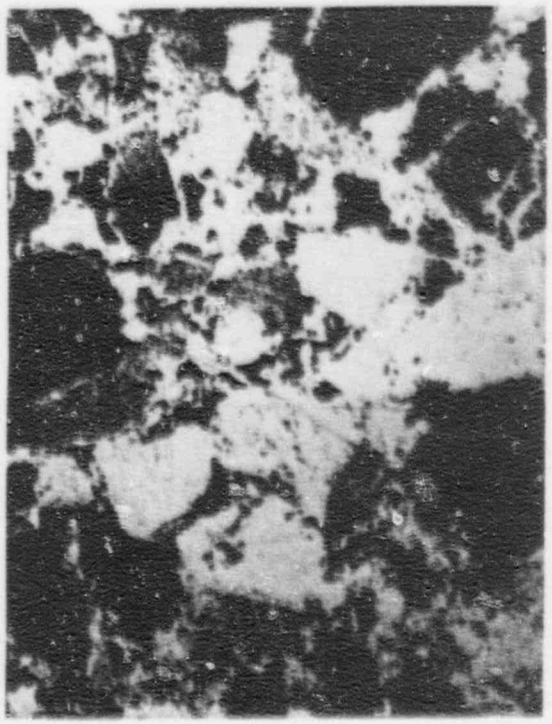

94.5x

89.8% TD

94.5x

90.8% TD

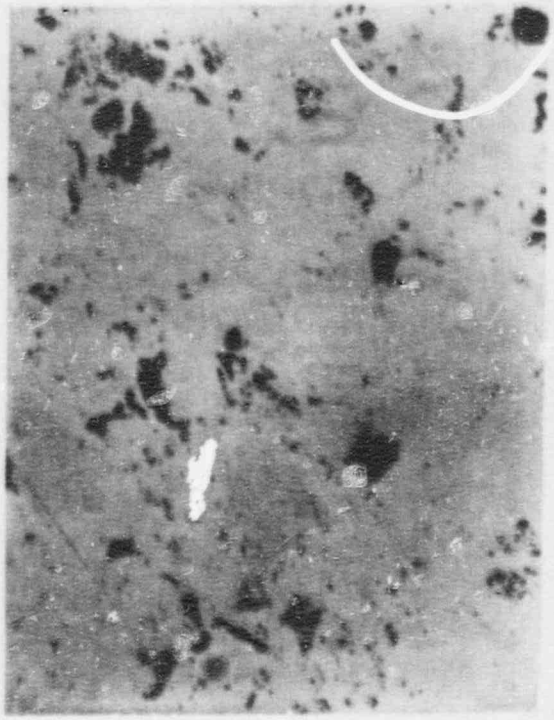

94.5x

93.3% TD

Fig. 3. UO_2 sintered to various densities at 1410°C

10,000 X

As-Sintered - 96.8% TD

Fig. 4. SEM photograph of sintered UO_2.

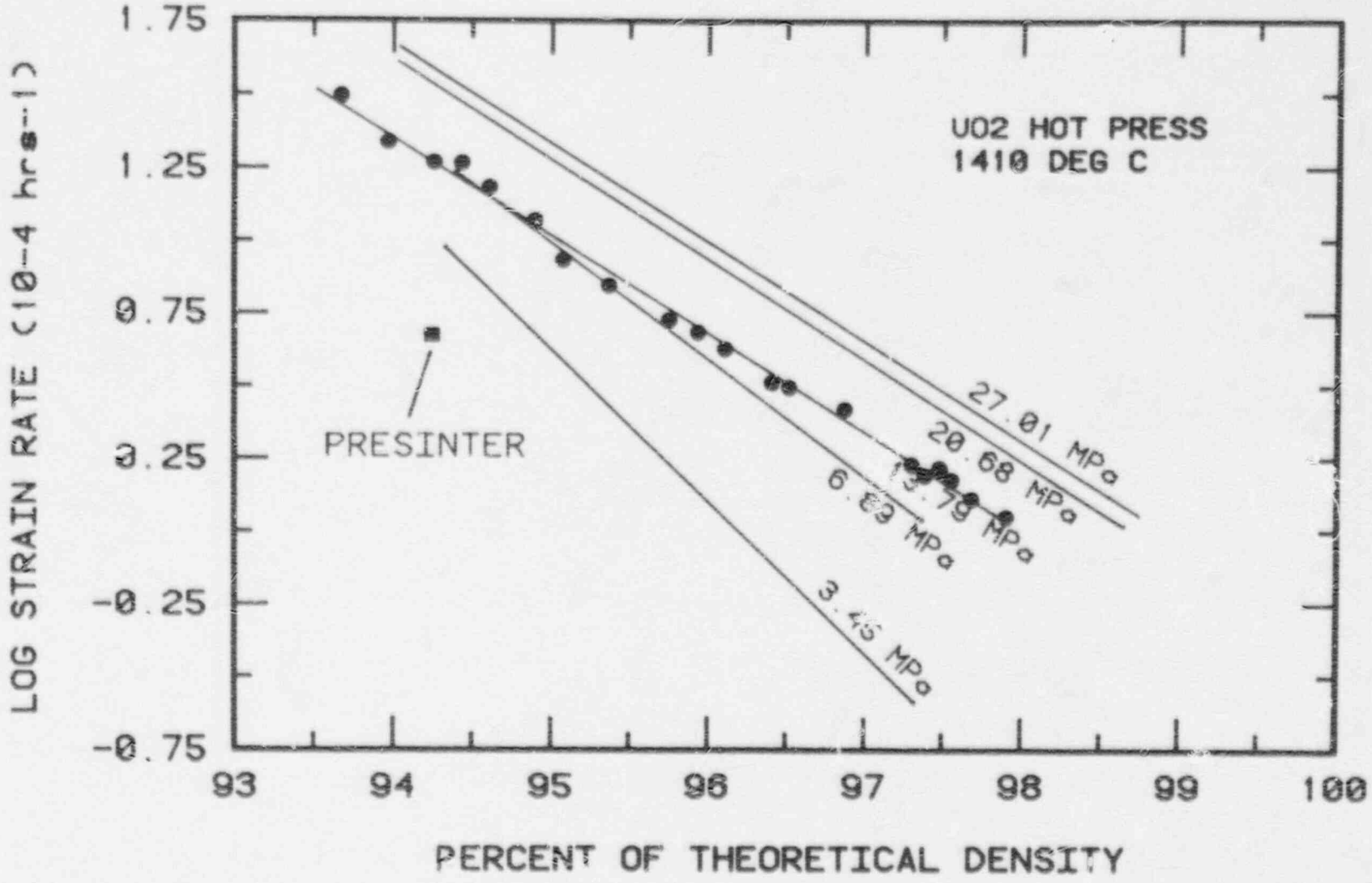

Fig. 5. Hot-pressing of UO_2 at various pressures

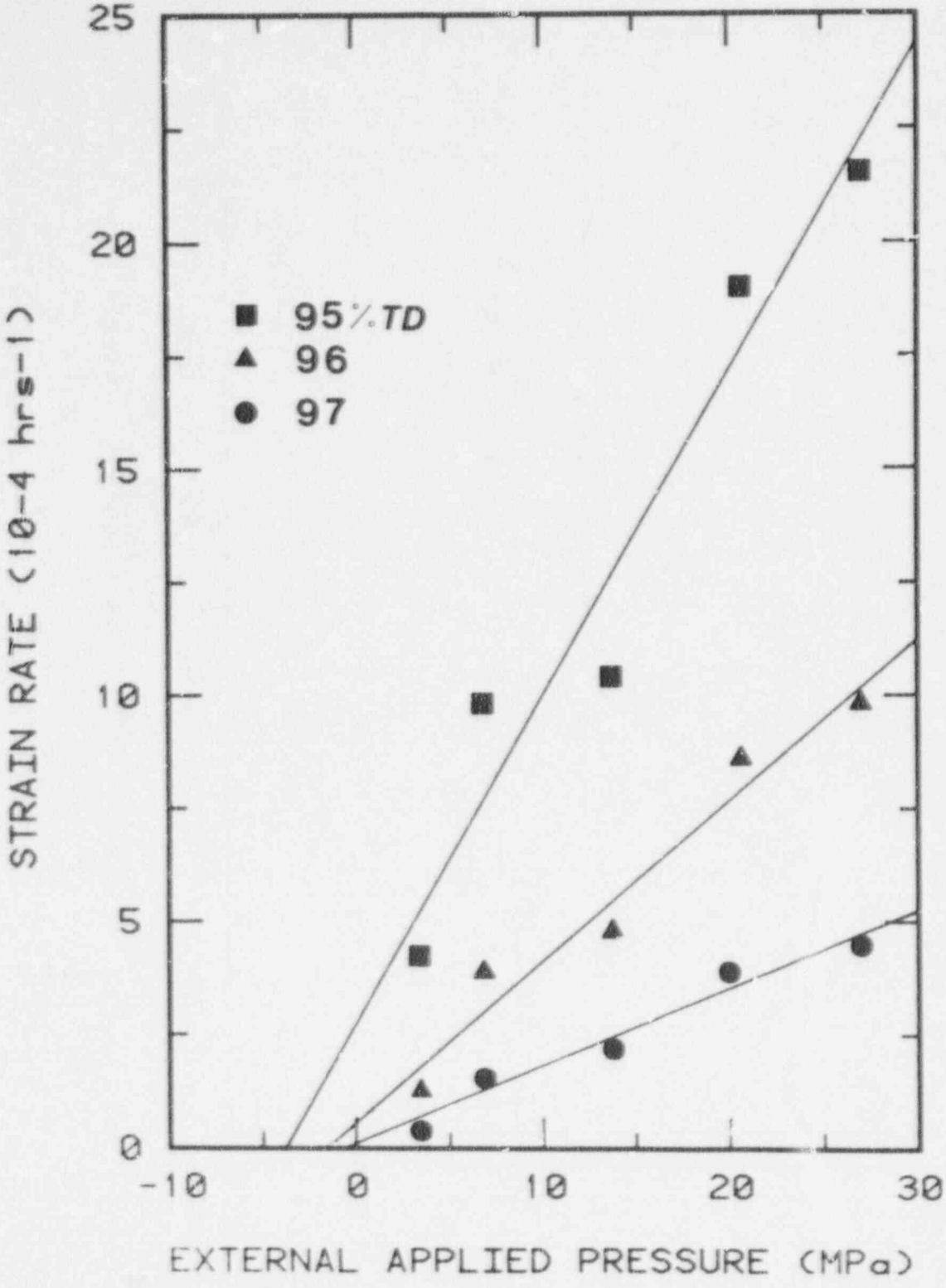

Fig. 6. Hot-pressing rates at constant density and 1410°C

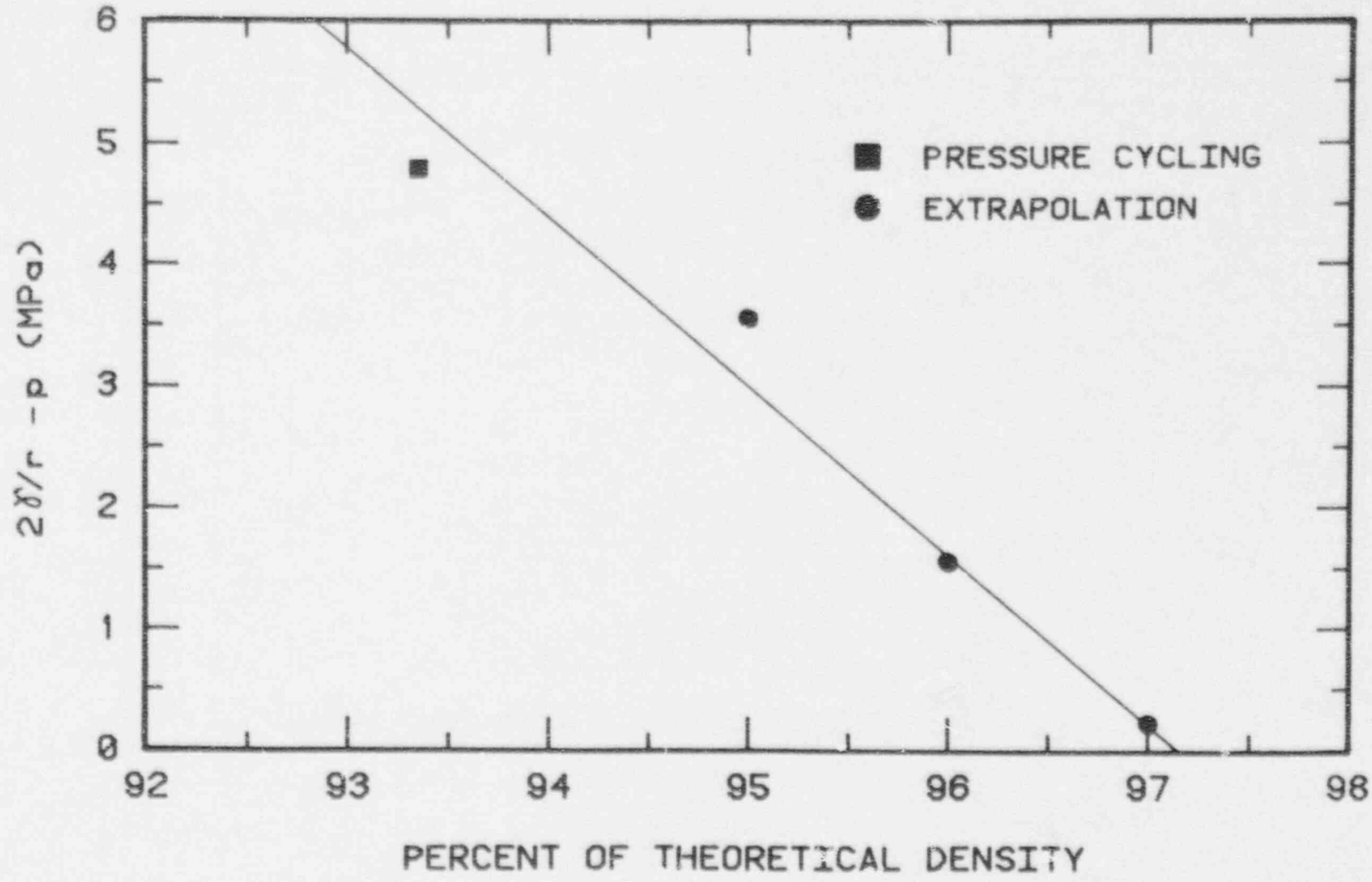

Fig. 7. Variation in surface tension and internal pressure with density at 1410°C

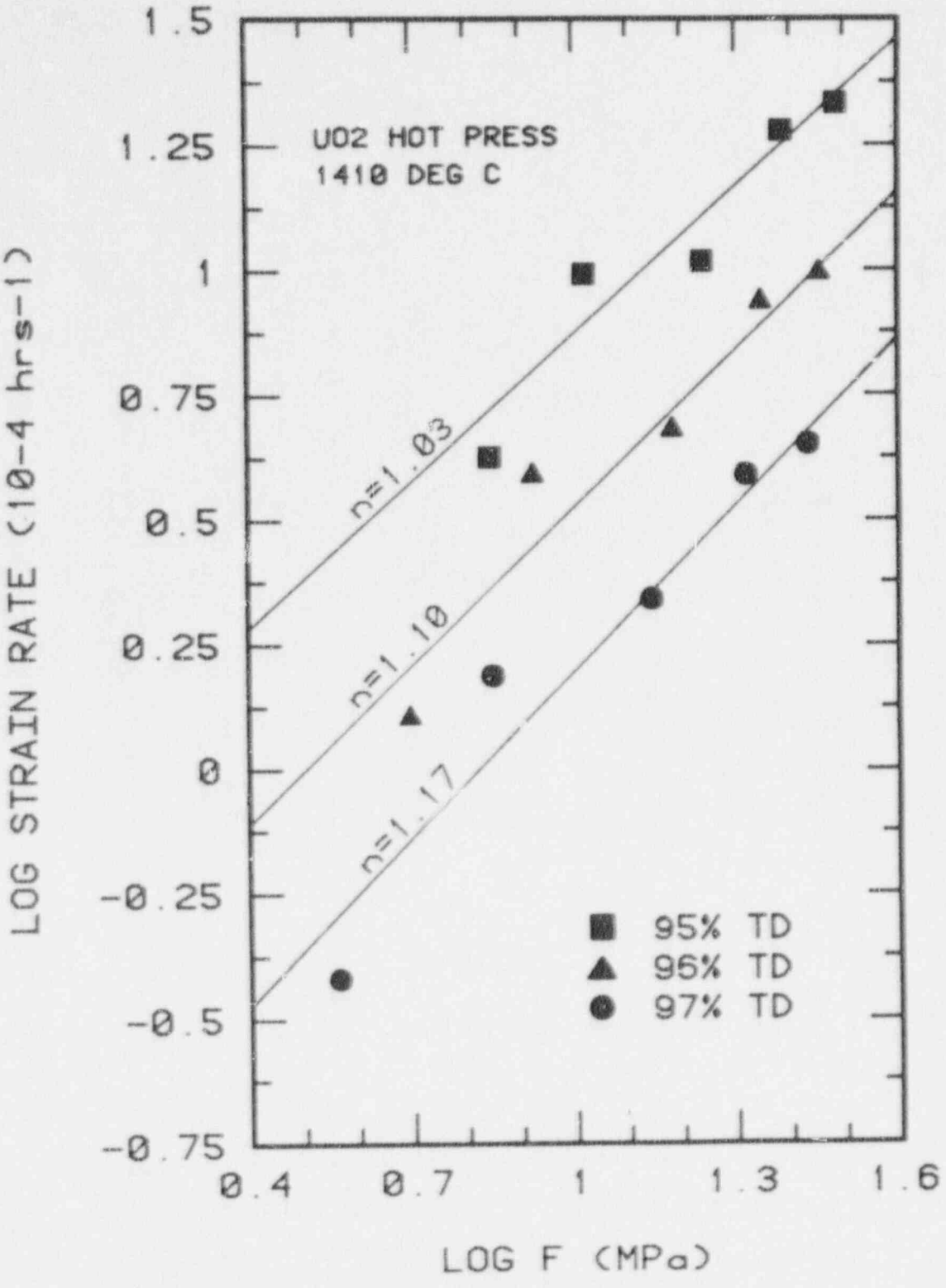

Fig. 8. Dependence of strain-rate on driving force

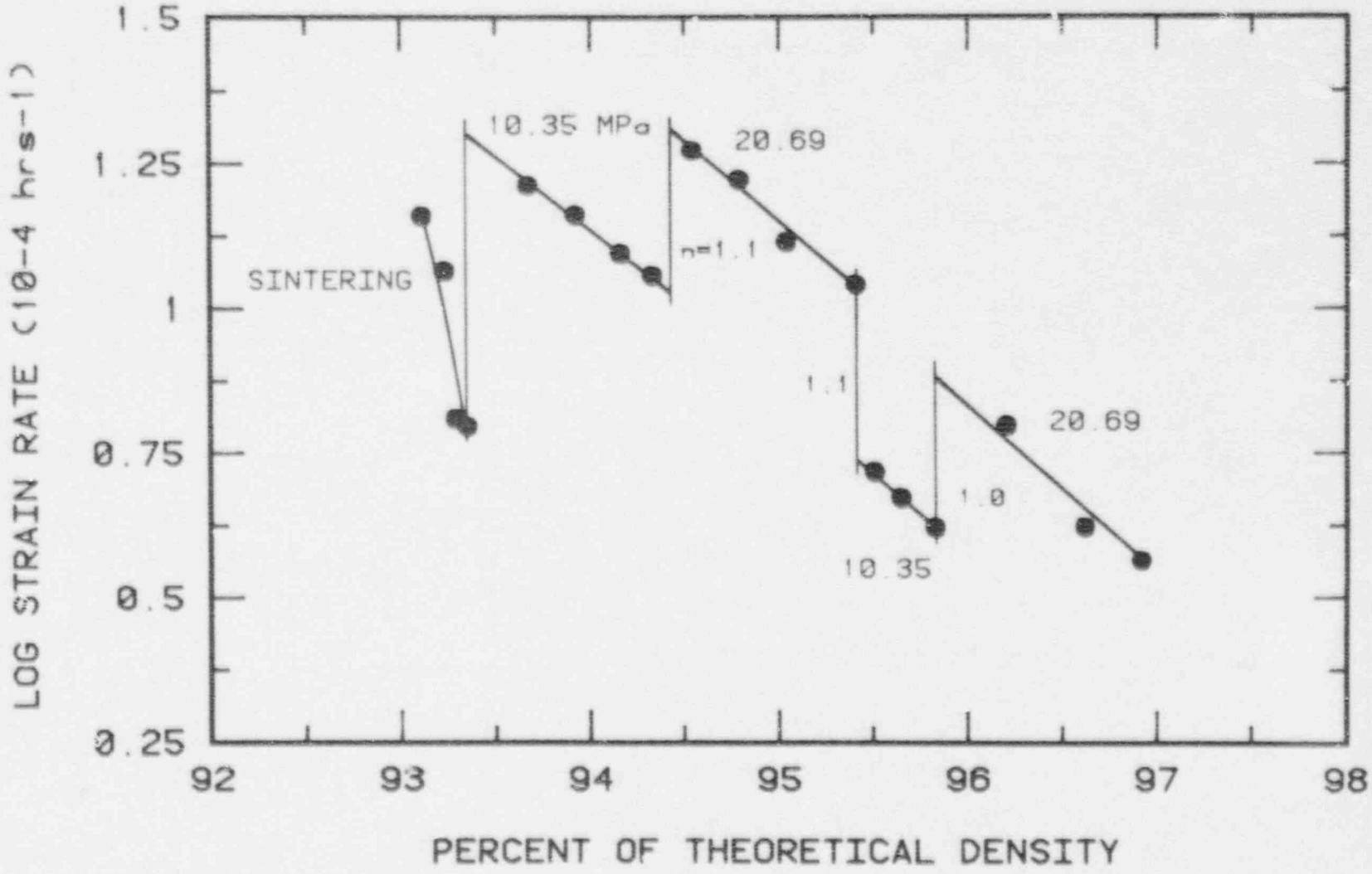

Fig. 9. Pressure cycling experiment

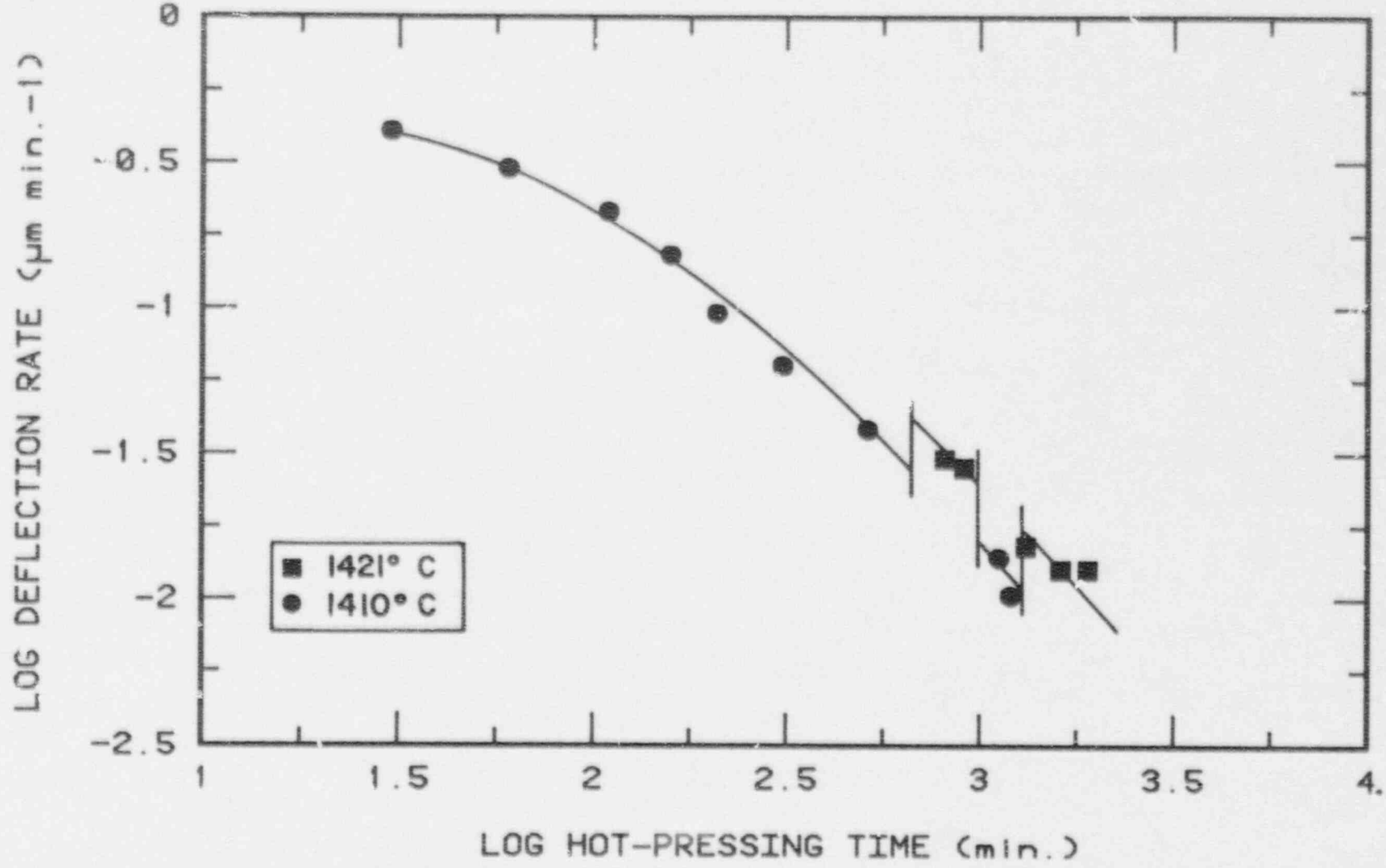

Fig. 10. Hot-pressing of UO_2 with temperature cycling.

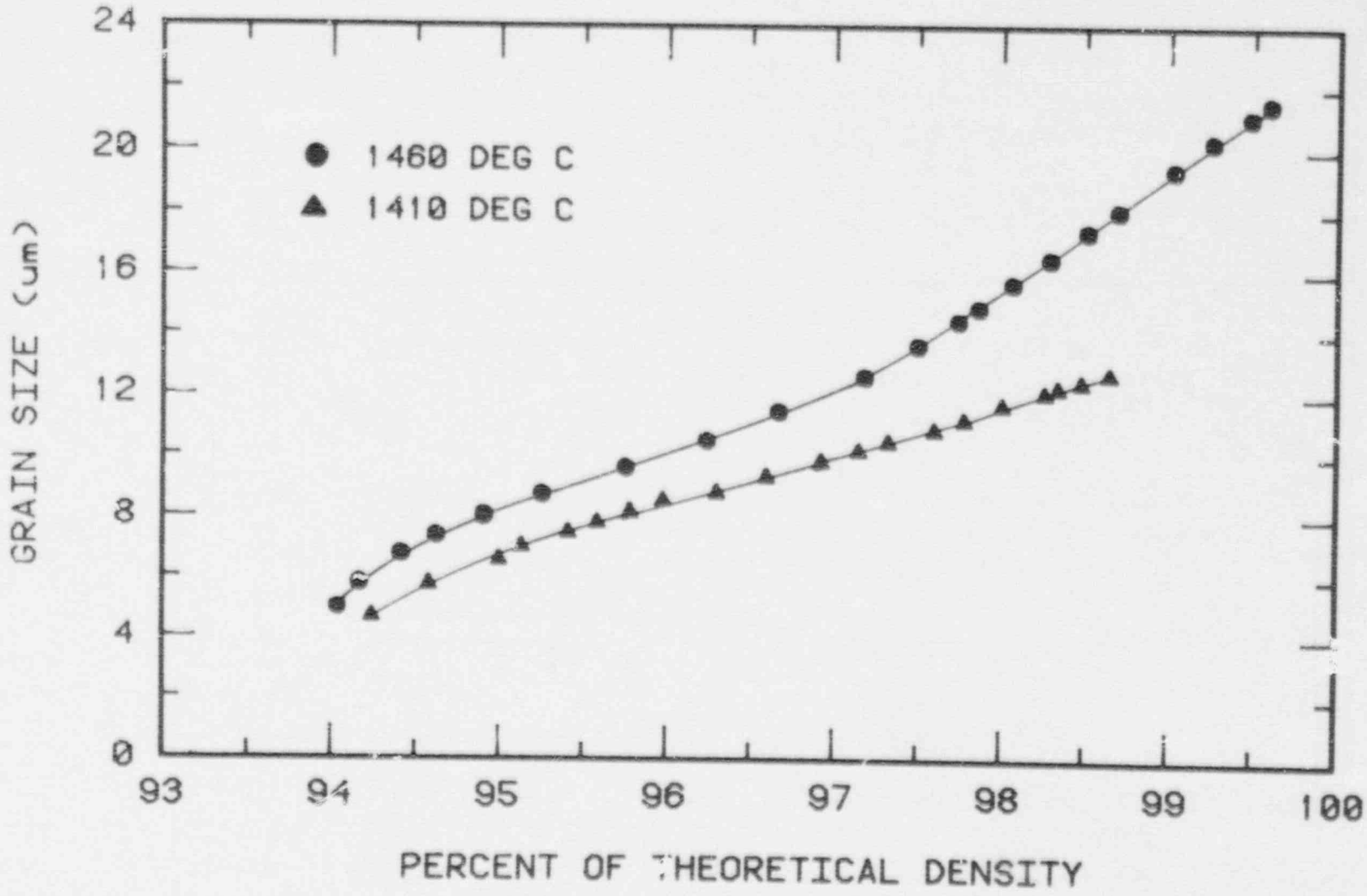

Fig. 11 Grain growth in UO_2 during hot-pressing at 1410°C and 1460°C

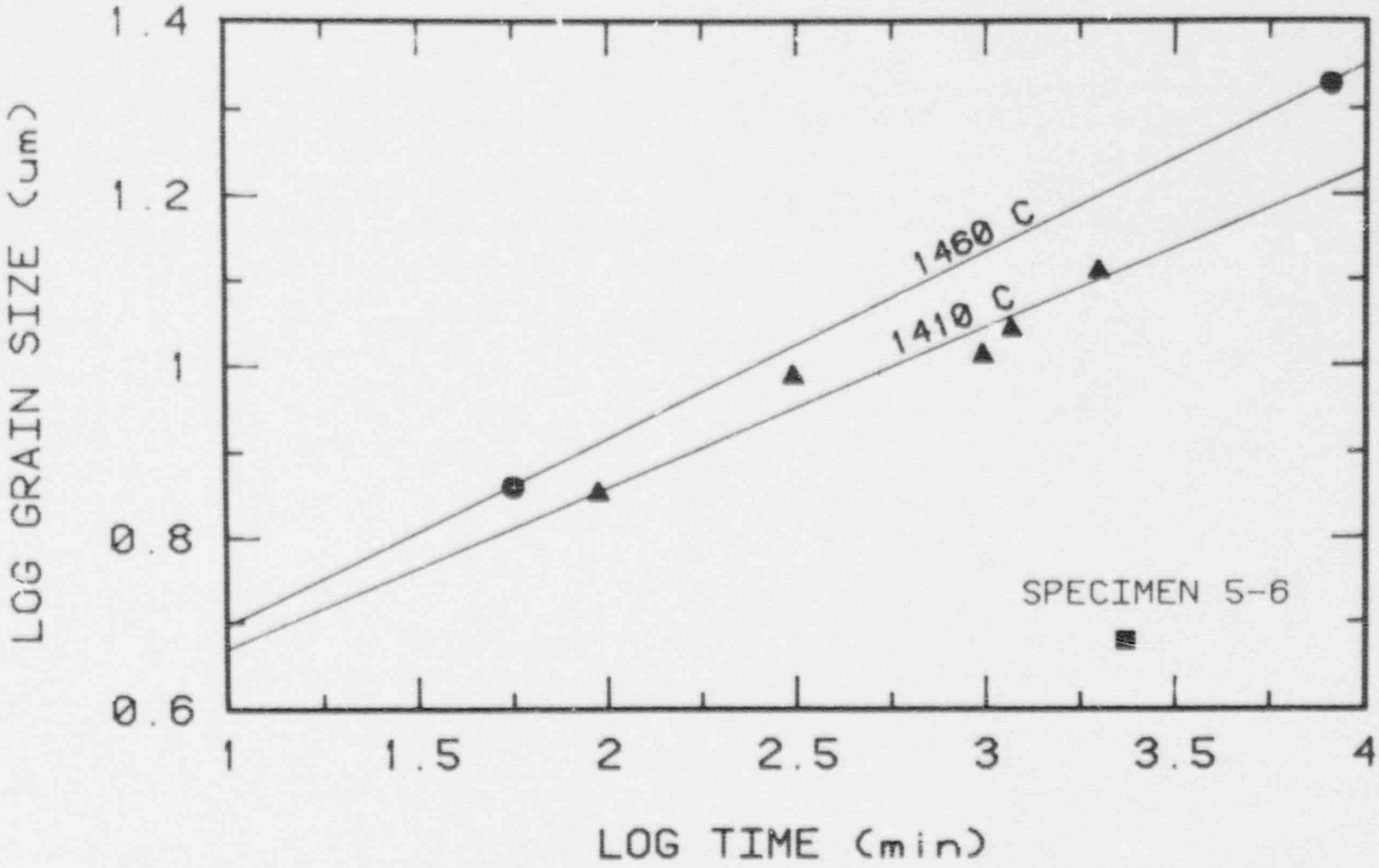

Fig. 12. Time dependence of grain growth during hot-pressing

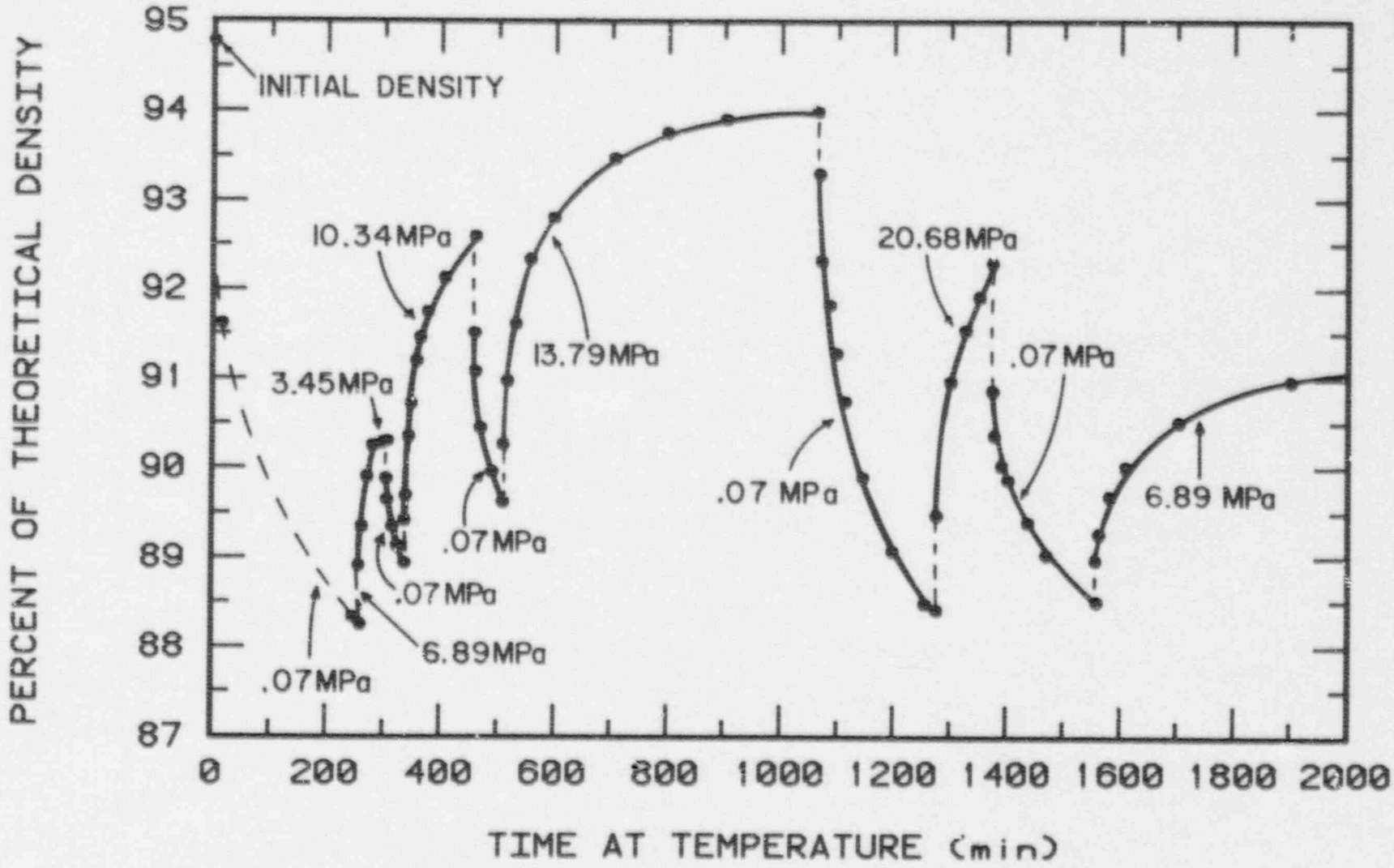

Fig. 13. Hot-pressing and swelling in sintered UO_2.

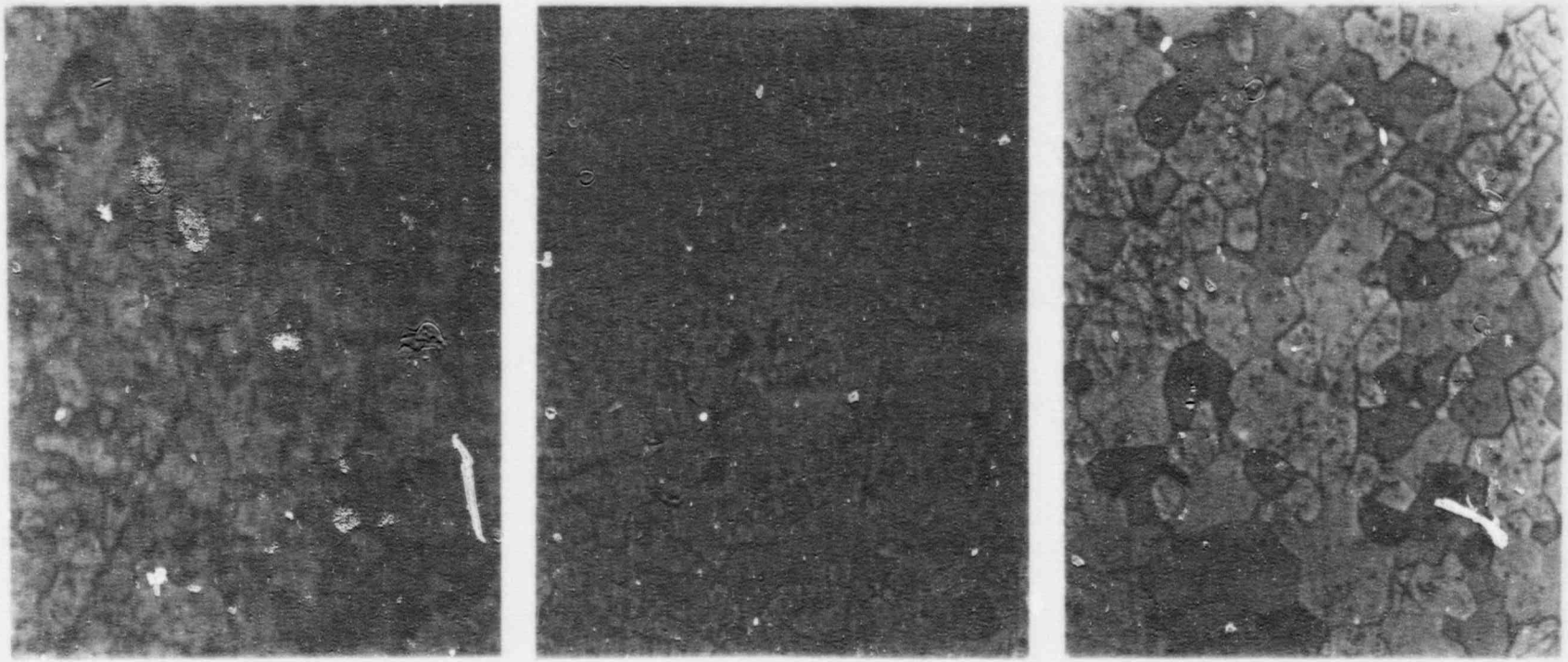

770x

As Sintered

1511°C/3 hrs.

93.3% TD

Hot-Pressed

1410°C/17 hrs.

96.9% TD

1410/33 hrs.

98.1 TD

Fig. 14. As-sintered and hot-pressed UO_2

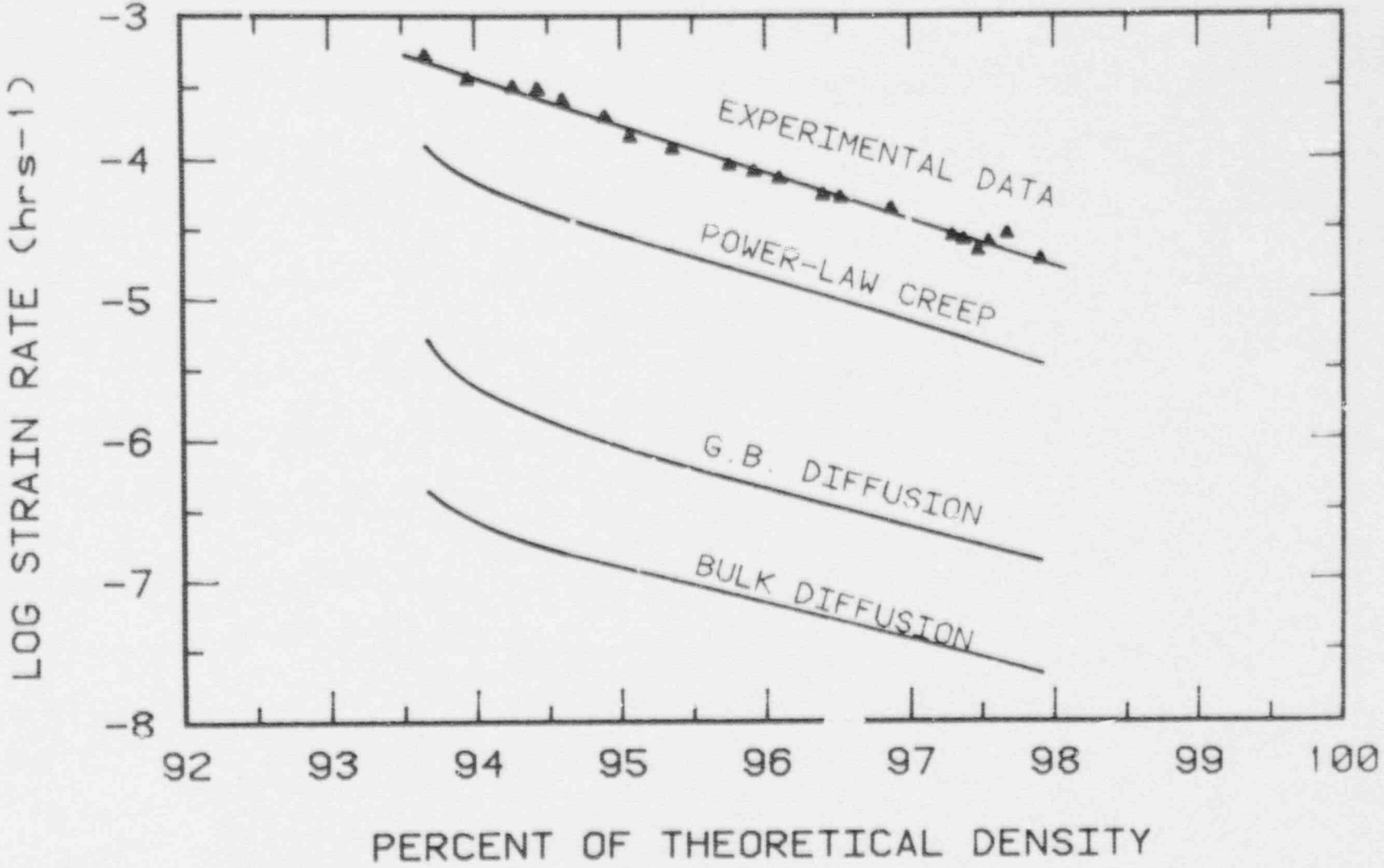

Fig. 15. Comparison of the results with various models

NRC FORM 335 (7-77)

U.S. NUCLEAR REGULATORY COMMISSION

BIBLIOGRAPHIC DATA SHEET

1. REPORT NUMBER (Assigned by DDC)
NUREG/CR-2023
PUR-101

4. TITLE AND SUBTITLE (Add Volume No., if appropriate)
Modelling Hot-Pressing of UO_2

2. (Leave blank)

3. RECIPIENT'S ACCESSION NO.

7. AUTHOR(S)
A. A. Solomon, K. M. Cochran, J. A. Habermeyer

5. DATE REPORT COMPLETED
MONTH: August YEAR: 1980

9. PERFORMING ORGANIZATION NAME AND MAILING ADDRESS (Include Zip Code)
School of Nuclear Engineering
Purdue University
West Lafayette, Indiana 47907

DATE REPORT ISSUED
MONTH: March YEAR: 1981

6. (Leave blank)

8. (Leave blank)

12. SPONSORING ORGANIZATION NAME AND MAILING ADDRESS (Include Zip Code)
U.S. Nuclear Regulatory Commission
Division of Reactor Safety Research
Office of NUclear Regulatory Research
Washington, D.C. 20555

10. PROJECT/TASK/WORK UNIT NO.

11. CONTRACT NO.
FIN B6313

13. TYPE OF REPORT
Technical Report

PERIOD COVERED (Inclusive dates)
N/A

15. SUPPLEMENTARY NOTES

14. (Leave blank)

16. ABSTRACT (200 words or less)

Final state isostatic hot-pressing of nearly stoichimetric UO_2 was investigated. The rate of hot-pressing is linearly dependent on the pressure driving force $F=P+\frac{2\gamma}{r}-p$, where P and p are the external and internal pressures, respectively, γ is the average surface energy and r is average pore radius. The apparent activation energy for hot-pressing agrees with that for U bulk diffusion. Grain growth during hot-pressing follows $d \propto t^n$, where d is the grain diameter, t is time and $n \simeq 0.2$. Grain size is also a function of temperature at constant density. The results indicate that Nabarro-Herring creep is the controlling mechanism of hot-pressing over the range of variables investigated, although the applicability of this model is questioned. The results also show that sintered UO_2 can entrap gas that can lead to swelling. For modelling purposes, the isostatic hot-pressing of UO_2, under the conditions investigated, is best described by,

$$\frac{1}{V}\frac{dV}{dt} = \frac{A_2}{d}\left(\frac{1-\rho}{\rho}\right)(\exp - Q/RT)\,F$$

where, $\frac{1}{V}\frac{dV}{dt}$ is the volumetric strain-rate in sec^{-1}, $A=8\times10^3$, d is in μm, ρ is the relative density, Q=480 kJ/g-mole, RT has its usual meaning, and F is in Pascals.

17. KEY WORDS AND DOCUMENT ANALYSIS

Hot-pressing
Swelling
UO_2
sintering

17a. DESCRIPTORS
N/A

17b. IDENTIFIERS/OPEN-ENDED TERMS
N/A

18. AVAILABILITY STATEMENT
Unlimited

19. SECURITY CLASS (This report)
Unclassified

21. NO. OF PAGES

20. SECURITY CLASS (This page)
Unclassified

22. PRICE
$

NRC FORM 335 (7-77)